CHEMISTRY OF MATERIALS

VOLUME 20, NUMBER 18 SEPTEMBER 23, 2008

Communications

Synthesis and Use of Tris(trimethylsilyl)antimony for the Preparation of InSb Quantum Dots

Christopher M. Evans, Stephanie L. Castro,
James J. Worman, and Ryne P. Raffaelle*

NanoPower Research Laboratories, Rochester Institute of Technology, Rochester, New York, and, Ohio Aerospace Institute, Cleveland, Ohio

Received October 3, 2007
Revised Manuscript Received July 8, 2008

Semiconductor quantum dots (QDs) have shown great potential for biological labeling[1] as well as in optoelectronic devices.[2−5] These applications have utilized the size-dependent properties of QDs, which allows for precise tuning of their optical properties. Predominately, II−VI QDs have been used in many recent applications because of the availability of countless synthetic procedures and high quantum yields. However, III−V QDs emerge as ideal candidates for many applications due to their large exciton Bohr radii (34 and 53 nm for InAs and InSb, respectively)[6] and narrow bandgaps. This allows the III−V QD optical bandgap to be tuned across a very large energy range, expanding from the mid-IR to UV. Additionally, research into biocompatible QDs has motivated several groups to forego using cadmium-, selenium-, or tellurium-containing nanocrystals in favor of III−V materials for health and environmental considerations.[7]

Currently, solution-phase synthetic approaches to nanocrystalline III−V QDs have relied upon dehalosilyation,[8−10] metathesis,[11,12] single-source precursors,[13,14] or hydrothermal processes.[15] Reaction schemes involving metathesis or single-source precursors typically require high temperatures (>400 °C) or reaction times up to several days[12] and yield polydisperse nanocrystals with very little size control. Conversely, dehalosilyation reactions and colloidal methods have provided good diameter control and yield highly crystalline QDs at lower temperatures and shorter times. These methodologies have been applied to the synthesis of several III−V semiconducting QDs such as: InP,[8−10] InAs,[10] $GaInP_2$,[9] and GaP.[9] However, synthetic progress has lacked in other III−V systems such as GaSb and InSb, mostly because of the absence of an appropriate antimony-containing precursor.

---

* Corresponding author. E-mail: rprsps@rit.edu.

(1) Ballou, B.; Lagerholm, B. C.; Ernst, L. A.; Bruchez, M. P.; Waggoner, A. S. *Bioconjugate Chem* **2004**, *15*, 79–86.

(2) Nozik, A. J. *Inorg. Chem.* **2005**, *44*, 6893–6899.

(3) Huynh, W. U.; Dittmer, J. J.; Alivisatos, A. P. *Science* **2002**, *295*, 2425–2427.

(4) Colvin, V. L.; Schamp, M. C.; Alivisatos, A. P. *Nature* **2000**, *370*, 354–357.

(5) Chakrabarti, S.; Holub, M. A.; Bhattacharya, P.; Mishima, T. D.; Santos, M. B.; Johnson, M. B.; Blom, D. A. *Nano Lett.* **2005**, *5*, 209–212.

(6) Trindade, T.; O'Brian, P.; Pickett, N. L. *Chem. Mater.* **2001**, *13*, 3843–3858.

(7) Bharali, D. J.; Lucey, D. W.; Jayakumar, H.; Pudavar, H. E.; Prasad, P. N. *J. Am. Chem. Soc.* **2005**, *127*, 11364–11371.

(8) Xu, S.; Kumar, S.; Nann, T. *J. Am. Chem. Soc.* **2006**, *128*, 1054–1055.

(9) Micic, O. I.; Sprague, J. R.; Curtis, C. J.; Jones, K. M.; Machol, J. L.; Nozik, A. J.; Giessen, H.; Fluegel, B.; Mohs, G.; Peyghambarian, N. *J. Phys. Chem.* **1995**, *99*, 7754–7759.

(10) Battaglia, D.; Peng, X. *Nano Lett.* **2002**, *2*, 1027–1030.

(11) Treece, R. E.; Macala, G. S.; Rao, L.; Franke, D.; Eckert, H.; Kaner, R. B. *Inorg. Chem.* **1993**, *32*, 2745–2752.

(12) Kher, S. S.; Wells, R. L. *Chem. Mater.* **1994**, *6*, 2056–2062.

(13) Foos, E. E.; Jouet, R. J.; Wells, R. L.; Rheingold, A. L.; Liable-Sands, L. M. *J. Organomet. Chem.* **1999**, *582*, 45–52.

(14) Foos, E. E.; Wells, R. L.; Rheingold, A. L. *J. Cluster Sci.* **1999**, *10*, 121–131.

(15) Lu, J.; Wei, S.; Yu, W.; Zhang, H.; Qian, Y. *Inorg. Chem.* **2004**, *43*, 4543–4545.

10.1021/cm702856v CCC: $40.75

Scheme 1. Synthetic Pathway to Tris(trimethylsilyl)antimony

$$\mathrm{Na} + (\mathrm{C_{10}H_8}) \rightarrow \mathrm{Na^+[C_{10}H_8]^{\cdot -}}$$

$$3\mathrm{Na^+[C_{10}H_8]^{\cdot -}} + \mathrm{Sb} \rightarrow \mathrm{Na_3Sb} + \mathrm{C_{10}H_8}$$

$$\mathrm{Na_3Sb} + 3\mathrm{(Cl)Si(CH_3)_3} \rightarrow \mathrm{Sb[Si(CH_3)_3]_3} + 3\mathrm{NaCl}$$

The synthesis of tris(trimethylsilyl)antimony, $\mathrm{(TMS)_3Sb}$, was first reported by Amberger and Salazar.[16] The experimental procedure involved the condensation of liquid ammonia over elemental lithium and antimony, followed by silyation to generate the desired product. In this report, we present results on the synthesis, isolation, and characterization of tris(trimethylsilyl)antimony and its utility as a precursor for antimony-containing quantum dots. This experimental procedure does not require the use of liquid ammonia, but instead uses commonly available organic solvents. The availability and proper characterization of a suitable precursor will enable researchers to further develop synthetic procedures yielding high-quality nanocrystalline III−V QDs.

$\mathrm{(TMS)_3Sb}$ was produced according to a reaction Scheme 1, in which $\mathrm{Na_3Sb}$ is an intermediate. The synthesis of $\mathrm{Na_3Sb}$ was adapted from a similar procedure used to generate sodium phosphide[17] that determined it was necessary to use an aromatic solvent for the production of $\mathrm{Na_3P}$. The necessity of aromaticity can possibly be explained by the formation of a donor−acceptor complex from a one-electron reduction of the aromatic species by the alkali metal.[18] Such complexes have been shown to increase the reaction rates for reductions of many transition metal complexes.[19] For the production of $\mathrm{Na_3Sb}$, it is unclear whether the donor−acceptor complex is actively participating as an intermediate in the formation of the antimony salt or merely acting as a catalyst, assisting in the reduction of the metallic antimony. In either case, it appears as though the formation of such a complex may be essential in the reaction mechanism associated with the production of sodium antimonide. Aromatic solvents alone were not sufficient to produce appreciable yields. It was only after the addition of a catalytic amount of naphthalene to the aromatic solvent that total yields of greater than 50% were realized.

To complete the reaction, $\mathrm{Na_3Sb}$ is silyated by the addition of three equivalents of chlorotrimethylsilane. Several reaction byproducts were observed (i.e., trimethylsilyl-naphthalene and benzyltrimethylsilane) in low quantity ($<1\%$) by MS analysis. However, these byproducts were easily removed by fractional distillation, allowing for the isolation of a colorless product with $>50\%$ yield. Upon exposure to air/moisture, $\mathrm{(TMS)_3Sb}$ quickly decomposed by combustion. Verification of structure was made by mass spectroscopy and nuclear magnetic resonance spectroscopy.

The MS data shown in Figure 1 represent a fragmentation pattern consistent with the desired structure.[20] The best evidence for the chemical composition is clearly seen in the inset of Figure 1. Here, the isotope pattern of the parent peak (*m*/*z* 340) is presented and can be compared to the calculated pattern. An excellent match between the experimental and theoretically predicted MS data was observed indicating that that the correct elemental composition was obtained. To observe this match, it was necessary to account for the abundances of the naturally occurring isotopes of not only the two antimony (^{121}Sb 57% and ^{123}Sb 43%) and three silicon isotopes (^{28}Si 92%, ^{29}Si 5%, and ^{30}Si 3%), but also the carbon and hydrogen isotopes as well.

Additional characterization of the compound by ^{1}H and ^{13}C NMR was performed and the results are consistent with the expected structure. A comparison of the chemical shift values for $\mathrm{(TMS)_3Sb}$ (δ ^{1}H 0.34 ppm, ^{13}C 5.1 ppm) to the phosphorus (0.28 ppm, 4.0 ppm) and arsenic analogues (0.30 ppm, 4.31 ppm[21]) reveals a clear trend. As the size of the anion increases ($\mathrm{P} < \mathrm{As} < \mathrm{Sb}$), the chemical shift for the methyl increases for both ^{1}H and ^{13}C. Additionally, the peak in the ^{1}H NMR spectrum exhibits coupling between the hydrogen and silicon nuclei analogous to tetramethylsilane. The coupling constant was measured to be 3 Hz, which is on the order of the coupling constant (6 Hz for tetramethylsilane) between the spin 1/2 ^{29}Si nuclei and a vicinal hydrogen.[22] Thus, the successful preparation of $\mathrm{(TMS)_3Sb}$ was demonstrated on the basis of spectroscopic data from both NMR and MS. This compound provided the first step in the development of a synthetic pathway to III−Sb QDs.

A colloidal synthetic pathway via transsilylation of $\mathrm{In(O_2CR)_3}$ with $\mathrm{(TMS)_3Sb}$ was investigated as a route to InSb QDs. Analogous to the procedures developed by Battaglia et al.,[10] as well as Lucey et al.,[23] we attempted to create colloidal dispersions of our group III ion. Unfortunately, it was determined that indium oxides are insufficiently soluble with any of the desired ligands. This necessitated the use of indium acetate, which would readily dissolved in a host of ligands, including fatty acids. $\mathrm{(TMS)_3Sb}$ dispersed in trioctylphosphine was quickly injected into the colloidal dispersion at an elevated temperature. The burst of nucleation was readily apparent upon injection by the immediate color change from transparent to yellow. Growth quickly followed and was evident by the slow change of color from yellow through the visible region eventually turning black. After cooling to room temperature, excess ligand and solvent were removed by sequential washings with methanol and hexanes, yielding a stable suspension of InSb QDs in hexanes. The product was soluble in nonpolar solvents such as hexanes and toluene, but insoluble in polar solvents such as methanol (inset Figure 2). Analysis of the soluble nanocrystals by absorption and fluorescence spectroscopy is shown in Figure

---

(16) Amberger, E.; G.; Salazar, R. W. *J. Organomet. Chem.* **1967**, *8*, 111–114.

(17) Peterson, D. J.; Logan, T. J. *J. Inorg. Nucl. Chem.* **1966**, *28*, 53–60.

(18) Micha-Screttas, M.; Heropoulos, G. A.; Steele, B. R. *J. Chem. Soc., Perkin Trans. 2* **1999**, *7*, 1443–1446.

(19) Grigoriev, V. A.; Cheng, D.; Hill, C. L.; Weinstock, I. A. *J. Am. Chem. Soc.* **2001**, *128*, 5292–5307.

(20) The parent peak is observed at *m*/*z* 340 with fragmentations resulting from the loss of a methyl group at *m*/*z* 325, a methyl and a TMS group at *m*/*z* 252, and two TMS groups and a methyl at *m*/*z* 179.

(21) Wells, R. L.; Self, M. F.; Johansen, J. D.; Laske, J. A.; Aubuchon, S. R.; Jones, L. J. *Inorg. Synth.* **1997**, *31*, 150–158.

(22) Silverstein, R. M.; Webster, F. X. *Spectrometric Identification of Organic Compounds*, 6th ed.; John Wiley & Sons: New York, 1998.

(23) Lucey, D. W.; MacRae, D. J.; Furis, M.; Sahoo, Y.; Cartwright, A. N.; Prasad, P. N. *Chem. Mater.* **2005**, *17*, 3754.

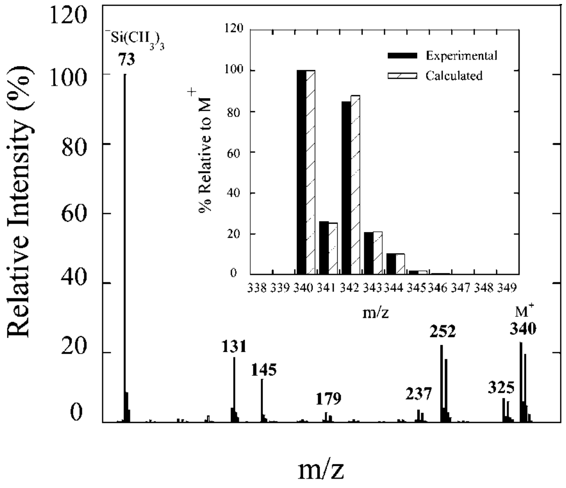

Figure 1. Electron impact mass spectroscopy of (TMS)$_3$Sb. (Inset) Isotope patterning of parent peak compared to the calculated patterning for the pure compound.

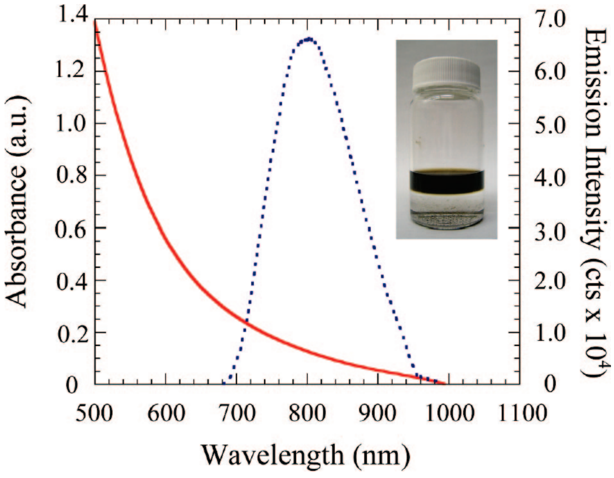

Figure 2. Band-edge emission (dashed) and absorption (solid) for InSb QDs with a diameter distribution centered at ~6 nm. (inset) InSb QDs show good solubility in organic solvents, such as hexanes, but are completely insoluble in methanol. The emission spectra were acquired using 475 nm excitation.

2. The slow "turn-on" of the absorption edge coupled with the 100 nm (233 meV) emission fwhm in the photoluminescene spectrum in the range of 700−1000 nm indicates that we have quantum confined InSb nanoparticles, but that sample size is somewhat polydisperse. This polydispersity would account for the broad absorption profile and lack of other distinct excitonic absorption peaks. Despite the polydispersity, the emission has been shifted greatly from 0.17 eV (7294 nm), where band-edge emission occurs in bulk InSb, indicating strong quantum confinement arising from its nanoscale dimensions.

Analytical expressions have been developed to correlate nanocrystal size to optical bandgap.[24] Commonly referred to as the Brus equation, this methodology has found widespread use for a variety of semiconductors. Typically, this expression has been applied to absorption data that best measure the lowest excited-state energy that this model relies upon. However, the lack of resolved features in the absorbance spectra convolves the analysis and necessitates the use of the photoluminescence data. On the basis of the emission range for our sample (Figure 2), we calculated a diameter distribution encompasing 8.3 and 9.5 nm. Unlike small exciton Bohr radii semiconductors (i.e., CdSe, ZnS, etc.,...), InSb undergos a large bandgap shifts for very small size variations. Therefore, realistic diameter distributions (~10%) will result in broadened optical features perhaps obscurring them completely. This result demonstrates the potential for controllable tuning of emission spanning the MID-IR to visible region by varying the particle size within this material system. However, special attention to diameter distributions will be necessary to produce spectrally narrow emission.

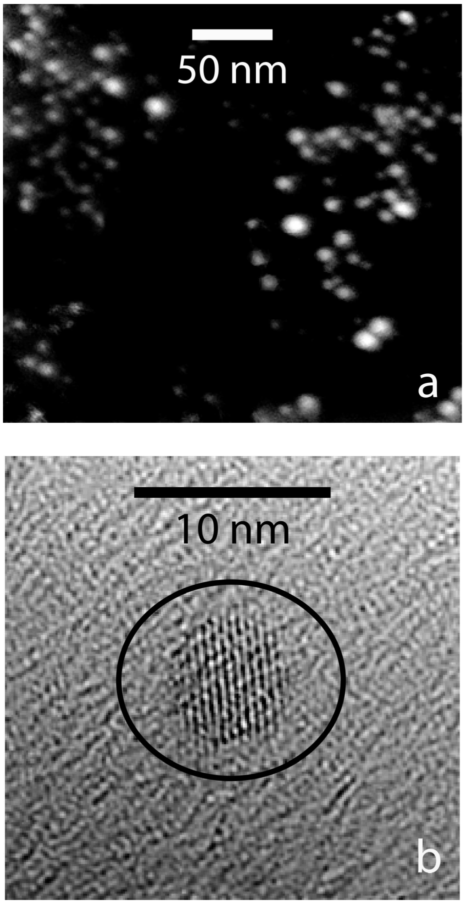

Figure 3. (a) STEM image of InSb quantum dots and (b) single InSb QDs showing individual lattice planes.

To verify the size distribution and crystallinity of our product, we performed TEM by drop casting a QD suspension onto a lacey carbon TEM grid. The polydispersity indicated by the optical spectroscopy was confirmed via STEM analysis as shown in Figure 3a. QD sizes can be seen to range between 3 and 13 nm with an average of 6 nm. Additionally, the crystalline nature of the product was evident upon imaging individual nanocrystals. Individual lattice planes are clearly resolvable for the QD shown in Figure 3b. It has been suggested that electron-beam-induced crystallization can occur and therefore TEM images do not represent unequivocal substantiation of crystallinity. However, our TEM images are consistent with optical data demonstrating large confinement energies (which would not be expected

---

(24) Steigerwald, M. L.; Brus, L. E. *Acc. Chem. Res.* **1990**, *23*, 183–188.

for an amorphous material) and support the crystalline nature of the product.

As an additional verification that the nanocrystals observed were in fact InSb, their elemental composition was determined using energy-dispersive spectroscopy (EDS; see the Supporting Infomation). After averaging several scans across varying areas of the sample, the ratio of indium to antimony was determined to be 1.05:1.00. The EDS and TEM data coupled with the spectroscopic results are strong evidence for the successful preparation of InSb quantum dots.

In summary, a synthetic procedure was developed for the preparation of tris(trimethylsilyl)antimony. $(TMS)_3Sb$ was utilized as a precursor in a colloidal synthetic approach to prepare InSb quantum dots. Characterization of the QDs by TEM and EDS verified their nanoscale dimensions, crystallinity, and composition. A large shift from the bulk bandgap (0.17 eV) to the near-IR (1.55 eV) was observed and is consistent with expected quantum confinement based on their size. This work provides a new synthetic pathway for the preparation of III−Sb QDs, which should enable new studies of their fundamental physical and chemical properties and perhaps improved optoelectronic devices.

Acknowledgment. The authors thank Jonathan Cowen from Case Western Reserve University for acquiring the TEM images. Additionally, we acknowledge the financial support for this work provided by BP Solar and the NASA Glenn Research Center (Grant NAG3-2595).

Supporting Information Available: Further experimental details and additional EDS characterization of InSb QDs (PDF). This material is available free for charge via the Internet at http://pubs.acs.org.

CM702856V